



## Original articles

# The translation operator. Applications to nonlinear reconstruction operators on nonuniform grids

S. Amat<sup>a,1</sup>, P. Ortiz<sup>a,1</sup>, J. Ruiz<sup>a,1</sup>, J.C. Trillo<sup>a,\*,1</sup>, D.F. Yáñez<sup>b,2</sup><sup>a</sup> *Departamento de Matemática Aplicada y Estadística, Universidad Politécnica de Cartagena, Spain*<sup>b</sup> *Departamento de Matemáticas, Universidad de Valencia, Spain*

Received 15 October 2021; received in revised form 17 March 2022; accepted 26 May 2022

Available online 17 June 2022

## Abstract

In this paper, we define a translation operator in a general form to allow for the application of the weighted harmonic mean in different applications. We outline the main steps to follow to define adapted methods using this tool. We give a practical example by improving the behavior of a nonlinear reconstruction operator defined in nonuniform grids, which was initially meant to work well with strictly convex data. With this improvement, the reconstruction can be now applied to data coming from smooth functions, retaining the expected maximum approximation order even around the inflection point areas, and maintaining convexity properties of the initial data. This adaptation can be carried out for general nonuniform grids, although to get the theoretical results about the approximation order, we require to work with quasi-uniform grids. We check the theoretical results through some numerical experiments.

© 2022 The Author(s). Published by Elsevier B.V. on behalf of International Association for Mathematics and Computers in Simulation (IMACS). This is an open access article under the CC BY license (<http://creativecommons.org/licenses/by/4.0/>).

*Keywords:* Interpolation; Reconstruction operator; Nonlinearity; Nonuniform grids; Approximation order; Convexity

## 1. Introduction

A high quantity of reconstruction operators have emerged in the last decades to attend to the demands of diverse applications in applied mathematics and industry [2,3,13,14]. Normally, polynomials are considered because of their simplicity and fast computation, and more specifically piecewise polynomials to avoid using high degree polynomials. High order polynomials involve larger stencils to build the reconstructions, which makes them more vulnerable to be affected by the presence of potential discontinuities in the data, apart from being well known for producing spurious maxima and minima known as Runge phenomena.

\* Corresponding author.

*E-mail addresses:* [sergio.amat@upct.es](mailto:sergio.amat@upct.es) (S. Amat), [portiz@navantia.es](mailto:portiz@navantia.es) (P. Ortiz), [juan.ruiz@upct.es](mailto:juan.ruiz@upct.es) (J. Ruiz), [jc.trillo@upct.es](mailto:jc.trillo@upct.es) (J.C. Trillo), [dionisio.yanez@uv.es](mailto:dionisio.yanez@uv.es) (D.F. Yáñez).

<sup>1</sup> The first four authors have been supported through the Proyecto financiado por la Comunidad Autónoma de la Región de Murcia, Spain a través de la convocatoria de Ayudas a proyectos para el desarrollo de investigación científica y técnica por grupos competitivos, incluida en el Programa Regional de Fomento de la Investigación Científica y Técnica (Plan de Actuación 2018) de la Fundación Séneca-Agencia de Ciencia y Tecnología de la Región de Murcia 20928/PI/18 and by the Spanish national research project PID2019-108336GB-I00.

<sup>2</sup> This author has been supported by grant PID2020-117211GB-I00 funded by MCIN/AEI/10.13039/501100011033, Spain.

<https://doi.org/10.1016/j.matcom.2022.05.031>

0378-4754/© 2022 The Author(s). Published by Elsevier B.V. on behalf of International Association for Mathematics and Computers in Simulation (IMACS). This is an open access article under the CC BY license (<http://creativecommons.org/licenses/by/4.0/>).

Nonlinear reconstructions allow adaptation to the available data and they also permit the preservation of certain properties inherent to the initial data. One of such properties is convexity, which is intimately related to curve and surface design. In this context, some nonlinear operators have appeared in the literature in the past few years [4–6,9,10,15]. In particular, we pay attention to the Piecewise Polynomial Harmonic (PPH) reconstruction [5,7,17,21,22,25], which was defined in nonuniform grids to preserve the convexity of the initial data under certain restrictions [22]. This reconstruction works well with data coming from strictly convex functions, but it fails to guarantee the approximation order in the vicinity of inflection points. This drawback comes directly from the heart of the definition itself of the PPH reconstruction operator, that is, the use of the weighted harmonic mean of two positive quantities. However, the problem can be solved by using a modified mean with a translation strategy.

In this paper, we introduce the definition of what we call a translation operator. We give a more general definition of the translation operator than the one that appears in [9], which deals with only two variables. This translation strategy can be applied in different fields to solve the problem of applying the harmonic mean whenever one of the arguments has different sign than another one or is null. As an example, we give some hints on how to define nonlinear adapted reconstructions which use this strategy and keep the required order of approximation. In particular, we apply this operator to the weighted harmonic mean obtaining a new adapted mean which retains similar properties as the original one, which is a crucial issue to be inserted into the construction of the improved PPH reconstruction operator. Our main concern about improving the approximation order around inflection points is to generate a tool that retains the approximation order in the whole domain for smooth functions and maintains local convexity in the convex areas. This convexity preservation property in smooth areas was proven in [22] under certain constraints. Also in [22] is made evident that the PPH reconstruction, both in uniform and in nonuniform grids, is relevant not only as an adapted reconstruction for smooth functions with isolated jump discontinuities (see [5,23]) but as a reconstruction that preserves convexity of the initial data.

We study several possible options for the translation operator to work in combination with the PPH reconstruction operator. In particular, we define a new way of choosing the best option depending on the specific data to which it is going to be applied. Part of this work has been inspired by the ideas given in [9].

Recent works deal with nonlinear reconstruction methods and nonuniform grids in different fields such as the solution of hyperbolic conservation laws [12,16,18,19] and the application of subdivision schemes [1,11,20].

The paper is organized as follows: Section 2 is dedicated to giving the definition and to study the translation operator in the general case of  $n$  variables. In Section 3, we analyze the behavior of the improved PPH reconstruction operator concerning the approximation order. In Section 4, we give a new way of selecting the translation parameter depending on the data. In Section 5, we present some numerical tests to confirm the theoretical results. Finally, some conclusions are provided in Section 6.

## 2. The translation operator

Given  $n$  real values  $x_1, \dots, x_n$ , let us define the extended weighted harmonic mean  $\tilde{V}(x_1, \dots, x_n)$  as follows.

$$\tilde{V}(x_1, \dots, x_n) = \begin{cases} \frac{1}{\sum_{i=1}^n \frac{w_i}{x_i}} = \frac{\prod_{k=1}^n x_k}{\sum_{i=1}^n w_i \prod_{k \neq i}^n x_k}, & \text{if } x_i > 0 \ \forall i, \\ 0 & \text{otherwise.} \end{cases} \tag{1}$$

And the weighted arithmetic mean by,

$$M(x_1, \dots, x_n) = \sum_{i=1}^n w_i x_i. \tag{2}$$

For the sake of simplicity, let us call them  $\tilde{V}$  and  $M$  without making explicit reference to their arguments if it is not strictly needed.

These two means have very interesting properties that make them suitable for the definition of nonlinear reconstruction operators among other applications, see [22] for example, where their versions with two variables were used. There are two main properties of these means that we want to recall. Their proofs can be found in [8].

**Lemma 1.** Let  $x_i > 0, i = 1, \dots, n$  be  $n$  positive real numbers and  $w_i > 0, i = 1, \dots, n$  the corresponding weights with  $\sum_{i=1}^n w_i = 1$ . Then, the weighted harmonic mean  $\tilde{V}$  is bounded as follows

$$\tilde{V} \leq \frac{x_1}{w_1}.$$

**Lemma 2.** Let  $x_i > 0, i = 1, \dots, n$  be  $n$  positive real numbers and  $w_i > 0, i = 1, \dots, n$  the corresponding weights with  $\sum_{i=1}^n w_i = 1$ . If  $x_i = O(1), \forall i = 1, \dots, n,$  and  $|x_1 - x_i| = O(h), \forall i = 2, \dots, n,$  then, the weighted harmonic mean  $\tilde{V}$  and the weighted arithmetic mean  $M$  satisfy

$$|M - \tilde{V}| = O(h^2).$$

Lemma 1 is related to the quality of adaptation of the methods to the presence of potential singularities. Lemma 2 is related to maintaining the same approximation order in a new nonlinear method as in its linear counterpart, from which it has been derived.

It happens, as we will explain in a moment, that in practice, the arguments of the means may be of different signs, and then neither the harmonic mean nor its extended version  $\tilde{V}$  is performing as expected. In particular, Lemma 2 is no longer necessarily true. To solve this problematic behavior we introduce a newly adapted version of the weighted harmonic mean. We first give a more general definition of a translation operator  $T$ . In [9], the translation operator was used in the case of 2 variables for a specific problem in the field of nonlinear splines. Since harmonic means of several variables appear in many applications we find it useful to give a more general definition.

**Definition 1.** Given  $h > 0$ , a translation operator  $T$  is any function  $T : \mathbb{R}^n \rightarrow \mathbb{R}$  satisfying

1.  $T(0, \dots, 0) = 0$ ,
2.  $T(x_1, \dots, x_n) = T(\sigma(x_1), \dots, \sigma(x_n))$ , where  $\sigma$  is any permutation of  $n$  elements,
3.  $T(-x_1, \dots, -x_n) = -T(x_1, \dots, x_n)$ ,
4.  $sign(x_1 + T(x_1, \dots, x_n)) = \dots = sign(x_n + T(x_1, \dots, x_n)), \forall (x_1, \dots, x_n) \neq (0, \dots, 0)$ ,
5. if  $(x_1, \dots, x_n) \neq (0, \dots, 0)$ , with  $|s| = \max\{|x_1|, \dots, |x_n|\}$ ,
  - (a) if  $\exists s_1 : |s_1| = |s|, sign(s_1) \neq sign(s)$ ,  
then  $sign(x_1 + T(x_1, \dots, x_n)) > 0, \dots, sign(x_n + T(x_1, \dots, x_n)) > 0$ ,
  - (b) if  $\nexists s_1 : |s_1| = |s|, sign(s_1) \neq sign(s)$ ,  
then  $sign(x_1 + T(x_1, \dots, x_n))sign(s) > 0, \dots, sign(x_n + T(x_1, \dots, x_n))sign(s) > 0$ ,
6.  $\min\{|x_1 + T(x_1, \dots, x_n)|, \dots, |x_n + T(x_1, \dots, x_n)|\} = O(1), \forall (x_1, \dots, x_n) \neq (0, \dots, 0)$ .

Property 4 of Definition 1 avoids the division by zero in (1), eliminating the case in which the sign of the arguments does not coincide. This solves the inconveniences that generates reducing the mean to zero in expression (1). Property 5 guarantees that the translation is done towards the largest of the arguments in absolute value. Finally, property 6 will be needed to prove similar lemmas to Lemmas 1 and 2, what in turn will allow us to prove adaptation in case of discontinuities and full order accuracy in the case of applying the technique that we are going to describe to define new nonlinear reconstruction operators.

This translation operator could potentially be applied in several fields where the formulation of the problems brings arithmetic means into the scene. Let us explain for example how to use it for the definition of new adapted reconstruction operators. The steps would be the following,

1. Start with a linear reconstruction operator.
2. Rewrite it by making appear arithmetic means of divided differences (or any other smoothness indicator).  
Be sure that the terms affected by any potential singularity remain only in some of the arguments of the arithmetic mean, but not in all of them. At least one divided difference must be free of any singularity.
3. Substitute the arithmetic means for translated harmonic means.

We are now ready to present the adapted weighted harmonic mean. First, we need to extend to the  $n$  variable case the definitions of weighted arithmetic and harmonic means.

**Definition 2.** We define the translated weighted harmonic mean as,

$$J(x_1, \dots, x_n) = \tilde{V}(x_1 + T(x_1, \dots, x_n), \dots, x_n + T(x_1, \dots, x_n)) - T(x_1, \dots, x_n), \tag{3}$$

where  $T(x_1, \dots, x_n)$  is an appropriate translation operator.

For this new mean we can give the following technical lemmas.

**Lemma 3.** For all  $(x_1, \dots, x_n) \in \mathbb{R}^n$ , the  $J(x_1, \dots, x_n)$  mean satisfies  $J(-x_1, \dots, -x_n) = -J(x_1, \dots, x_n)$ .

**Proof.**

$$\begin{aligned} J(-x_1, \dots, -x_n) &= \tilde{V}(-x_1 + T(-x_1, \dots, -x_n), \dots, -x_n + T(-x_1, \dots, -x_n)) - T(-x_1, \dots, -x_n) \\ &= \tilde{V}(-(x_1 + T(x_1, \dots, x_n)), \dots, -(x_n + T(x_1, \dots, x_n))) + T(x_1, \dots, x_n) \\ &= -\tilde{V}(x_1 + T(x_1, \dots, x_n), \dots, x_n + T(x_1, \dots, x_n)) + T(x_1, \dots, x_n) = -J(x_1, \dots, x_n). \end{aligned}$$

□

From now on, we will drop the arguments of the translation operator  $T$  for the sake of simplicity. They are easily inferred by the context.

**Lemma 4.** For all  $(x_1, \dots, x_n) \in \mathbb{R}^n$ , the translated weighted harmonic mean is bounded as follows,

$$|J(x_1, \dots, x_n)| \leq \max \left\{ \frac{|x_1 + T|}{w_1}, |T| \right\}. \tag{4}$$

**Proof.** Since  $\tilde{V}(x_1 + T, \dots, x_n + T)$  and  $T$  have the same sign,

$$|J(x_1, \dots, x_n)| \leq \max \{ |\tilde{V}(x_1 + T, \dots, x_n + T)|, |T| \}.$$

According to [Lemma 1](#) we have that

$$|\tilde{V}(x_1 + T, \dots, x_n + T)| \leq \frac{|x_1 + T|}{w_1}.$$

Then,

$$|J(x_1, \dots, x_n)| \leq \max \left\{ \frac{|x_1 + T|}{w_1}, |T| \right\}.$$

□

**Lemma 5.** Let  $a > 0$  be a fixed positive real number,  $T$  be a translation operator, and let  $(x_1, \dots, x_n) \in \mathbb{R}^n$  be such that  $|x_i + T| \geq a, \forall i = 1, \dots, n$ . If  $|x_1 - x_i| = O(h), \forall i = 2, \dots, n$ , then the translated weighted harmonic mean is a second order approximation to the weighted arithmetic mean  $M(x_1, \dots, x_n) = \sum_{i=1}^n w_{x_i} x_i$ , i.e.,

$$|M(x_1, \dots, x_n) - J(x_1, \dots, x_n)| = O(h^2). \tag{5}$$

**Proof.** Using the definition of  $J(x_1, \dots, x_n)$  we get

$$\begin{aligned} |M(x_1, \dots, x_n) - J(x_1, \dots, x_n)| &= |M(x_1, \dots, x_n) - \tilde{V}(x_1 + T, \dots, x_n + T) + T| \\ &= |M(x_1 + T, \dots, x_n + T) - \tilde{V}(x_1 + T, \dots, x_n + T)|. \end{aligned}$$

and applying [Lemma 2](#) we have that

$$|M(x_1 + T, \dots, x_n + T) - \tilde{V}(x_1 + T, \dots, x_n + T)| = O(h^2).$$

□

Notice that [Lemmas 4](#) and [5](#) correspond to an extension of previous [Lemmas 1](#) and [2](#).

**Remark 1.** The bound obtained in Lemma 4 can be improved for particular choices of the translation  $T$ , due to the fact that in the general case, one applies the triangular inequality in the proof to reach the result, and this step can be refined for a given  $T$ . See for example the definition of the translation  $\tilde{T}$  in (6) and its corresponding Lemma 6.

We are going now to use this technique for the improvement of the nonlinear reconstruction PPH on nonuniform grids, see [22]. The new ingredient consists in the substitution of weighted harmonic means by their translated version. We start by using the above definition of a translation operator and previous lemmas in order to give a particular translation operator in the two variable case, which we will use in our numerical examples.

One possible definition of translation  $T$  fulfilling previous Definition 1 is obtained by

$$\tilde{T}(x, y) = \begin{cases} s \epsilon & \text{if } xy > 0, \\ s(\min\{|x|, |y|\} + \epsilon) & \text{otherwise,} \end{cases} \tag{6}$$

where  $\epsilon = O(1)$  is a constant and  $s$  is defined using the sign function as

$$s = \begin{cases} \text{sign}(y) & \text{if } |x| \leq |y|, \\ \text{sign}(x) & \text{otherwise.} \end{cases}$$

Notice that, we will also drop the arguments of the translation operator  $\tilde{T}$  for the sake of simplicity.

The proposed new mean is then given by

$$\tilde{J}(x, y) = \tilde{V}(x + \tilde{T}, y + \tilde{T}) - \tilde{T}, \tag{7}$$

and verifies the following specific lemma, which improves the bound in Lemma 4.

**Lemma 6.** For all  $(x, y) \in \mathbb{R}^2$ , the translated weighted harmonic mean  $\tilde{J}$  is bounded as follows

$$|\tilde{J}(x, y)| \leq \begin{cases} \frac{|x|}{w_x} + \frac{w_y}{w_x} \epsilon & \text{if } |x| \leq |y|, \\ \frac{|y|}{w_y} + \frac{w_x}{w_y} \epsilon & \text{otherwise.} \end{cases}$$

**Proof.** Let us suppose without loss of generality that  $|x| \leq |y|$ . We consider four possible different cases, and we prove the result separately for each case.

**Case A.**  $x \leq 0, y > 0$ . In this case  $\tilde{T} = -x + \epsilon > 0$ .

$$\tilde{J}(x, y) = \tilde{V}(\epsilon, y - x + \epsilon) + x - \epsilon.$$

Now, we observe that,

$$\tilde{V}(\epsilon, y - x + \epsilon) \geq \epsilon,$$

$$\tilde{V}(\epsilon, y - x + \epsilon) < \frac{1}{w_x} \epsilon.$$

If  $\tilde{V}(\epsilon, y - x + \epsilon) + x - \epsilon \geq 0$ ,

$$|\tilde{J}(x, y)| < |x| + \frac{w_y}{w_x} \epsilon.$$

If  $\tilde{V}(\epsilon, y - x + \epsilon) + x - \epsilon < 0$ ,

$$|\tilde{J}(x, y)| = \epsilon - x - \tilde{V}(\epsilon, y - x + \epsilon) \leq |x|.$$

**Case B.**  $x \geq 0, y < 0$ . In this case  $\tilde{T} = -x - \epsilon < 0$ .

$$\tilde{J}(x, y) = \tilde{V}(-\epsilon, y - x - \epsilon) + x + \epsilon.$$

Observing that

$$\tilde{V}(-\epsilon, y - x - \epsilon) \leq -\epsilon,$$

$$\tilde{V}(-\epsilon, y - x - \epsilon) > -\frac{1}{w_x} \epsilon.$$

If  $\tilde{V}(-\epsilon, y - x - \epsilon) + x + \epsilon \geq 0$ ,  
 $|\tilde{J}(x, y)| = \tilde{V}(-\epsilon, y - x - \epsilon) + x + \epsilon \leq |x|$ .  
 If  $\tilde{V}(-\epsilon, y - x - \epsilon) + x + \epsilon < 0$ ,  
 $|\tilde{J}(x, y)| \leq |x| + \frac{w_y}{w_x}\epsilon$ .

**Case C.**  $x > 0, y > 0$ . In this case  $\tilde{T} = \epsilon > 0$ .

$$\tilde{J}(x, y) = \tilde{V}(x + \epsilon, y + \epsilon) - \epsilon.$$

We are going to use that in this case,

$$\begin{aligned} \tilde{V}(x + \epsilon, y + \epsilon) &\geq x + \epsilon, \\ \tilde{V}(x + \epsilon, y + \epsilon) &< \frac{1}{w_x}(x + \epsilon). \end{aligned}$$

Since in this case  $\tilde{V}(x + \epsilon, y + \epsilon) - \epsilon \geq 0$ , then,

$$|\tilde{J}(x, y)| < \frac{|x|}{w_x} + \frac{w_y}{w_x}\epsilon.$$

**Case D.**  $x < 0, y < 0$ . In this case  $\tilde{T} = -\epsilon < 0$ .

$$\tilde{J}(x, y) = \tilde{V}(x - \epsilon, y - \epsilon) + \epsilon.$$

In this case using that,

$$\begin{aligned} \tilde{V}(x - \epsilon, y - \epsilon) &\leq x - \epsilon, \\ \tilde{V}(x - \epsilon, y - \epsilon) &> \frac{1}{w_x}(x - \epsilon), \end{aligned}$$

and observing that  $\tilde{V}(x - \epsilon, y - \epsilon) + \epsilon < 0$ , we get,

$$|\tilde{J}(x, y)| < \frac{|x|}{w_x} + \frac{w_y}{w_x}\epsilon.$$

□

### 3. Improved PPH reconstruction operator

In this section we introduce the modified mean defined in the previous section into the definition of the PPH reconstruction operator [22], giving rise to the following definition.

**Definition 3 (Translated PPH Reconstruction).** Let  $X = (x_i)_{i \in \mathbb{Z}}$  be a nonuniform mesh. Let  $f = (f_i)_{i \in \mathbb{Z}}$  be a sequence in  $l_\infty(\mathbb{Z})$ . Let  $D_j$  and  $D_{j+1}$  be the second order divided differences defined by,

$$\begin{aligned} D_j &:= f[x_{j-1}, x_j, x_{j+1}] = \frac{f_{j-1}}{h_j(h_j + h_{j+1})} - \frac{f_j}{h_j h_{j+1}} + \frac{f_{j+1}}{h_{j+1}(h_j + h_{j+1})}, \\ D_{j+1} &:= f[x_j, x_{j+1}, x_{j+2}] = \frac{f_j}{h_{j+1}(h_{j+1} + h_{j+2})} - \frac{f_{j+1}}{h_{j+1} h_{j+2}} + \frac{f_{j+2}}{h_{j+2}(h_{j+1} + h_{j+2})}, \end{aligned} \tag{8}$$

and for each  $j \in \mathbb{Z}$  let us consider the modified values  $\{\tilde{f}_{j-1}, \tilde{f}_j, \tilde{f}_{j+1}, \tilde{f}_{j+2}\}$  built according to the following rule,

- **Case 1:** If  $|D_j| \leq |D_{j+1}|$

$$\begin{cases} \tilde{f}_i = f_i, & j - 1 \leq i \leq j + 1, \\ \tilde{f}_{j+2} = \frac{-1}{\gamma_{j,2}}(\gamma_{j,-1}f_{j-1} + \gamma_{j,0}f_j + \gamma_{j,1}f_{j+1}) + \frac{J_j}{\gamma_{j,2}}, \end{cases} \tag{9}$$

• **Case 2:** If  $|D_j| > |D_{j+1}|$

$$\begin{cases} \tilde{f}_{j-1} = \frac{-1}{\gamma_{j,-1}}(\gamma_{j,0}f_j + \gamma_{j,1}f_{j+1} + \gamma_{j,2}f_{j+2}) + \frac{J_j}{\gamma_{j,-1}}, \\ \tilde{f}_i = f_i, \quad j \leq i \leq j + 2, \end{cases} \tag{10}$$

where  $\gamma_{j,i}$ ,  $i = -1, 0, 1, 2$  are given by,

$$\begin{aligned} \gamma_{j,-1} &= \frac{h_{j+1} + 2h_{j+2}}{2h_j(h_{j+1} + h_j)(h_j + h_{j+1} + h_{j+2})}, \\ \gamma_{j,0} &= \frac{1}{2h_{j+1}(h_j + h_{j+1} + h_{j+2})} \left( \frac{h_{j+1} + 2h_j}{h_{j+1} + h_{j+2}} - \frac{h_{j+1} + 2h_{j+2}}{h_j} \right), \\ \gamma_{j,1} &= \frac{1}{2h_{j+1}(h_j + h_{j+1} + h_{j+2})} \left( \frac{h_{j+1} + 2h_{j+2}}{h_{j+1} + h_j} - \frac{h_{j+1} + 2h_j}{h_{j+2}} \right), \\ \gamma_{j,2} &= \frac{1}{2h_{j+2}(h_{j+1} + h_{j+2})(h_j + h_{j+1} + h_{j+2})}, \end{aligned} \tag{11}$$

with  $h_i = x_{i+1} - x_i$ , and  $J_j = J(D_j, D_{j+1})$ , with  $J$  the translated weighted harmonic mean defined in (3) or in (7) with the weights  $w_{j,0}$  and  $w_{j,1}$  given by,

$$\begin{aligned} w_{j,0} &= \frac{h_{j+1} + 2h_{j+2}}{2(h_j + h_{j+1} + h_{j+2})}, \\ w_{j,1} &= \frac{h_{j+1} + 2h_j}{2(h_j + h_{j+1} + h_{j+2})} = 1 - w_{j,0}. \end{aligned} \tag{12}$$

We define the translated PPH nonlinear reconstruction operator as,

$$PPHT(x) = PPHT_j(x), \quad x \in [x_j, x_{j+1}], \tag{13}$$

where  $PPHT_j(x)$  is the unique third degree interpolation polynomial which satisfies,

$$PPHT_j(x_i) = \tilde{f}_i, \quad j - 1 \leq i \leq j + 2. \tag{14}$$

The coefficients for this new reconstruction operator match exactly with the coefficients of the original PPH reconstruction except for the substitution of  $\tilde{V}_j = \tilde{V}(D_j, D_{j+1})$  for  $J_j$ .

We can prove now the following result about the order of approximation attained by the reconstruction. We want to point out that the order improves in the vicinity of inflection points due to the considered translation, which is an improvement with respect to the original reconstruction procedure, see Theorem 1 in [23].

We are going to study the approximation order of the given reconstruction for functions of class  $C^4(\mathbb{R})$  with an isolated jump discontinuity at a given point  $\mu$ . We consider only the case of working with  $\sigma$  quasi-uniform grids, according to the following definition.

**Definition 4.** A nonuniform mesh  $X = (x_i)_{i \in \mathbb{Z}}$  is said to be a  $\sigma$  quasi-uniform mesh if there exist  $h_{min} = \min_{i \in \mathbb{Z}} h_i$ ,  $h_{max} = \max_{i \in \mathbb{Z}} h_i$ , and a finite constant  $\sigma$  such that  $\frac{h_{max}}{h_{min}} \leq \sigma$ .

The next theorem proves full order of accuracy, that is fourth order of accuracy, in all intervals except the interval containing the singularity and the two adjacent intervals. We observe that the approximation order is reduced to second-order in the two adjacent intervals, but it is not completely lost.

**Theorem 1.** Let  $f(x)$  be a function of class  $C^4(\mathbb{R} \setminus \{\mu\})$ , with a jump discontinuity at the point  $\mu$ . Let  $X = (x_i)_{i \in \mathbb{Z}}$  be a  $\sigma$  quasi-uniform mesh in  $\mathbb{R}$ , with  $h_i = x_i - x_{i-1}$ ,  $\forall i \in \mathbb{Z}$ , and  $f = (f_i)_{i \in \mathbb{Z}}$ , the sequence of point values of the function  $f(x)$ ,  $f_i = f(x_i)$ . Let us consider  $j \in \mathbb{Z}$  such that  $\mu \in [x_j, x_{j+1}]$ . Then, the reconstruction  $PPHT(x)$  satisfies,

1. In  $[x_i, x_{i+1}]$ ,  $i \neq j - 1, j, j + 1$ , then

$$\max_{x \in [x_i, x_{i+1}]} |f(x) - PPHT(x)| = O(h^4).$$

2. In  $[x_{j-1}, x_j] \cup [x_{j+1}, x_{j+2}]$ ,

$$\max_{x \in [x_{j-1}, x_j] \cup [x_{j+1}, x_{j+2}]} |f(x) - PPHT(x)| = O(h^2),$$

where  $h = \max_{i \in \mathbb{Z}} \{h_i\}$ .

**Proof.** We do the proof point by point.

1. Given  $x \in [x_i, x_{i+1}]$ , the reconstruction operator is built as  $PPHT(x) = PPHT_i(x)$ .

We recall that second order divided differences amount to second order derivatives at an intermediate point divided by two, i.e.,

$$D_i = \frac{f''(\mu_1)}{2!}, \quad D_{i+1} = \frac{f''(\mu_2)}{2!},$$

with  $\mu_1 \in (x_{i-1}, x_{i+1})$  and  $\mu_2 \in (x_i, x_{i+2})$ . Due to the properties of the translation  $T$  in Definition 1, we have that,

$$D_i + \tilde{T} = O(1), \quad D_{i+1} + \tilde{T} = O(1) \text{ and } D_{i+1} - D_i = O(h),$$

and from Lemma 5 we get that,

$$M_i - \tilde{J}_i = \frac{w_{i,0}w_{i,1}(D_{i+1} - D_i)^2}{w_{i,0}D_{i+1} + w_{i,1}D_i + \tilde{T}} = O(h^2). \tag{15}$$

Using this information and the specific form of the coefficients  $a_{i,s}$  and  $\tilde{a}_{i,s}$   $s = 0, 1, 2, 3$ , of the cubic Lagrange interpolation polynomial and of the translated PPH reconstruction operator respectively, see [22], one can easily get that,

$$|\tilde{a}_{i,s} - a_{i,s}| = O(h^{4-s}), \quad s = 0, 1, 2, 3. \tag{16}$$

Thus,

$$|PPHT_i(x) - PL_i(x)| \leq \sum_{s=0}^3 |\tilde{a}_{i,s} - a_{i,s}| \left| \left(x - x_{i+\frac{1}{2}}\right)^s \right| = O(h^4),$$

where  $PL_i(x)$  is the Lagrange interpolatory polynomial. Taking into account again the triangular inequality,

$$|f(x) - PPHT_i(x)| \leq |f(x) - PL_i(x)| + |PL_i(x) - PPHT_i(x)| = O(h^4),$$

using that Lagrange interpolation also attains fourth order of accuracy.

2. In order to prove Point 2, let us suppose without loss of generalization, that  $x \in [x_{j-1}, x_j]$ . The other case is proven analogously. Since, by hypothesis, the function  $f(x)$  is smooth in  $[x_{j-2}, x_j]$  and it presents a jump discontinuity in the interval  $[x_j, x_{j+1}]$ , we have  $D_{j-1} = O(1)$  and  $D_j = O(1/h^2)$ . Therefore  $|D_{j-1}| \leq |D_j|$ .

Let  $PL2_{j-1}(x)$  be the second degree Lagrange interpolatory polynomial built using the three pairs of values  $(x_{j-2}, f_{j-2})$ ,  $(x_{j-1}, f_{j-1})$ ,  $(x_j, f_j)$ .

$$PL2_{j-1}(x) = \hat{a}_{j-1,0} + \hat{a}_{j-1,1} \left(x - x_{j-\frac{1}{2}}\right) + \hat{a}_{j-1,2} \left(x - x_{j-\frac{1}{2}}\right)^2,$$

where

$$\begin{aligned} \hat{a}_{j-1,0} &= \frac{f_{j-1} + f_j}{2} - \frac{h_j^2}{4} D_{j-1}, \\ \hat{a}_{j-1,1} &= \frac{-f_{j-1} + f_j}{h_j}, \\ \hat{a}_{j-1,2} &= D_{j-1}. \end{aligned} \tag{17}$$



The difference between these coefficients and the ones of  $PPHT_{j-1}(x)$ , see [22], is given by,

$$\begin{aligned} \tilde{a}_{j-1,0} - \hat{a}_{j-1,0} &= \frac{h_j^2}{4} (D_{j-1} - J_{j-1}), \\ \tilde{a}_{j-1,1} - \hat{a}_{j-1,1} &= \frac{h_j^2}{4h_{j-1} + 2h_j} (D_{j-1} - J_{j-1}), \\ \tilde{a}_{j-1,2} - \hat{a}_{j-1,2} &= -(D_{j-1} - J_{j-1}), \\ \tilde{a}_{j-1,3} &= -\frac{2}{2h_{j-1} + h_j} (D_{j-1} - J_{j-1}). \end{aligned} \tag{18}$$

Taking into account Eqs. (18), Lemma 4 and the triangular inequality we obtain,

$$\begin{aligned} |J_{j-1}(D_{j-1}, D_j)| &\leq \max\left\{\frac{1}{w_{j-1,0}} |D_{j-1} + T|, |T|\right\}, \\ |D_{j-1} - J_{j-1}| &\leq |D_{j-1}| + \max\left\{\frac{1}{w_{j-1,0}} |D_{j-1} + T|, |T|\right\} = O(1), \\ |\tilde{a}_{j-1,s} - \hat{a}_{j-1,s}| &= O(h^{2-s}), \quad s = 0, 1, 2, 3, \\ |PPHT_{j-1}(x) - PL2_{j-1}(x)| &\leq \sum_{s=0}^3 |\tilde{a}_{j-1,s} - \hat{a}_{j-1,s}| \left| \left(x - x_{j-\frac{1}{2}}\right)^s \right| = O(h^2), \\ |f(x) - PPHT_{j-1}(x)| &\leq |f(x) - PL2_{j-1}(x)| + |PL2_{j-1}(x) - PPHT_{j-1}(x)| = O(h^2). \end{aligned}$$

□

**Remark 2.** If one pays attention to the proof of point 2 in Theorem 1 and considers the definition of the particular translation proposed in (6) and Lemma 6, then it is easy to reach the conclusion that the smaller the  $\epsilon$  the better the accuracy obtained in the two intervals adjacent to the jump discontinuity. However, in order for the proof of point 1 to work,  $\epsilon$  must still be  $O(1)$ , so that it is possible to avoid the reduction of order close to inflection points where the second order divided differences could be  $O(h)$  and, therefore, Lemma 5 would not be applicable. A nonlinear choice of the value of  $\epsilon$  seems to be appropriate.

**Remark 3.** In the intervals adjacent to the jump discontinuity, one can get third order of accuracy in the cases where there is a change of sign between the two consecutive second divided differences involved in either  $[x_{j-1}, x_j]$  or  $[x_{j+1}, x_{j+2}]$ , just by considering a translation of the type  $\tilde{T}$  in (6) with an adapted value of  $\epsilon$ , small enough in those intervals, at least  $\epsilon = O(h)$ . In this cases we will have,

$$\max_{x \in [x_{j-1}, x_j] \cup [x_{j+1}, x_{j+2}]} |f(x) - PPHT(x)| = O(h^3).$$

The reason for this fact comes from the expression of the adapted mean  $\tilde{J}$  in these cases, Case A and Case B of Lemma 6, combined with the proof of the second point of Theorem 1 by estimating now the difference  $|D_{j-1} - J_{j-1}| = O(h)$ .

#### 4. Nonlinear choice of the parameter $\epsilon$ in the translation operator

It turns out that it is better to take a small  $\epsilon$  near a potential jump discontinuity, but it must remain  $O(1)$  at zones where there is the possibility of having second order divided differences  $D_i$  of order  $O(h)$ , just as it happens close to inflection points. This assessment is also observed in the numerical experiments.

This is the reason why we propose a strategy to choose  $\epsilon$  automatically depending on the data. Inspired by the smoothness indicators proposed in [9,24], see Remark 4, we propose an  $\epsilon$  with the following expression,

$$\epsilon_j := \frac{h_j^\alpha}{|D_j| + |D_{j+1}| + \xi}, \tag{19}$$

where  $\alpha := [\beta(|D_j| + |D_{j+1}|)]$  is the integer part of  $IS_j := \beta(|D_j| + |D_{j+1}|)$ , which stands as a kind of smoothness indicator. The parameter  $\xi = h^4$  is included to avoid divisions by zero. The parameter  $\beta$  is taken into account to make the  $\epsilon$  smaller as we get apart from the inflection points. This fact will result in obtaining a reconstruction

almost equal to the original PPH reconstruction in smooth areas without inflection points, allowing the preservation of convexity (see [22]). We have considered  $\beta = 1$  in our numerical experiments. The parameter  $\alpha$  is large when a jump discontinuity affects the stencil used to obtain it and, in turn, this situation will result in a very small value of  $\epsilon_j$  in that area. On the other hand, this indicator provides  $\alpha = 0$  near an inflection point for sufficiently small grid sizes and, therefore,  $\epsilon_j = O(h^{-r})$ , for some  $r > 0$ . Thus,  $\epsilon$  is guaranteed to be large in this region.

**Remark 4.** In [24] Jiang and Shu propose to obtain smoothness indicators using something similar to the total variation, but based on the  $L^2$  norm so that the result is smoother than the total variation. The proposed formula is just a sum of the  $L^2$  norms of the derivatives of the interpolation polynomials in the cell-averages over the interval  $(x_{j-1/2}, x_{j+1/2})$ . Those indicators are more related to the localization of critical points instead of inflection points. Moreover, for our case, expression (19) is cheaper computationally since  $D_j$  and  $D_{j+1}$  are already computed.

### 5. Numerical experiments

In this section, we present a simple numerical test to validate the theoretical results. Our experiment computes the approximation order of the considered reconstructions in several areas corresponding with the different points in Theorem 1. In particular, we measure the approximation order in the following areas, identified with the given symbols:

- $A_0$ : In the interval containing the jump discontinuity.
- $A_1$ : In a region where the function is smooth without inflection points and far away from them.
- $A_2$ : In a region where the function is smooth but contains an inflection point.
- $A_3$ : In a region close to the inflection point without containing it.
- $A_4$ : In the subinterval just to the right of the one containing the singularity.

We deal with the following piecewise polynomial reconstruction operators of third degree:

- Lagrange: piecewise centered Lagrange interpolation polynomial.
- PPH: nonlinear reconstruction operator given in [22].
- PPHT,  $\epsilon = 0.5$ : translated version of the PPH reconstruction operator given in Definition 3.
- PPHT,  $\epsilon = 0.05$ : translated version of the PPH reconstruction operator given in Definition 3.
- PPHT,  $\epsilon_j$ : translated version of the PPH reconstruction operator given in Definition 3 using an adaptive value of the parameter  $\epsilon$  according to expression (19).

Let  $X^0 = (0, 3, 8, 11, 17, 23, 25, 27, 31, 32, 36, 37.5, 38, 39.3, 40)\frac{\pi}{20}$  be a nonuniform grid in  $[0, 2\pi]$  and  $f(x)$  the following smooth function with a jump discontinuity at  $x = 1.2\pi$ , and an inflection point at  $x = \frac{3\pi}{2}$ ,

$$f(x) := \begin{cases} \sin x & x < 1.2\pi, \\ \cos x + 10 & x \geq 1.2\pi. \end{cases}$$

This function has also inflection points at  $x = 0, \pi$ , but we will be dealing with the indicated regions, letting aside those inflection points. The results for those cases give similar conclusions and they have not been reported. In fact, the numerical tests that have been carried out with different functions presenting well separated inflection points and isolated jump discontinuities give similar results as the one shown in this article. For example, if the jump size is smaller, then the approximation errors are in turn smaller, but the approximation orders present exactly the same behavior (maybe with the need for smaller grid sizes).

In our experiment we have taken for the grid  $X^0$  the following regions  $A_0^0 = [0, 2\pi]$ ,  $A_1^0 = [2, 3]$ ,  $A_2^0 = [4, 5]$ ,  $A_3^0 = [\frac{31\pi}{20}, 6.2]$ ,  $A_4^0 = [\frac{25\pi}{20}, 4]$ . Notice that these intervals correspond to the initial grid  $X^0$  and they need to vary appropriately among the scales  $k$  to satisfy the requirements of the definition of the associated region.

Given the initial abscissas  $x_i^0, i \in I_0 = \{0, \dots, 14\}$ , we consider the set of nested grids  $X^k = \{x_i^k\}_{i \in I^k}$ , where  $x_{2i}^k = x_i^{k-1}$ ,  $x_{2i+1}^k = \frac{x_i^{k-1} + x_{i+1}^{k-1}}{2}$ , and  $I^k = \{x_0^k, \dots, x_{n_k}^k\}$ ,  $k = 0, 1, \dots, 7$ , with  $n_k = 2n_{k-1} - 1$ ,  $n_0 = 14$ . For each level of resolution  $k$ , we build the corresponding reconstruction  $R_k(x)$  using the data  $(x_i^k, f(x_i^k)), i \in I_k$  computing the approximation errors in the infinity norm with respect to the original function using a denser set of abscissas, i.e., we compute a numerical approximation of,

$$E_k := \|f(x) - R_k(x)\|_\infty.$$

**Table 1**

Approximation errors  $E_k$  and approximation orders  $p$  in the infinity norm obtained at iteration  $k, k = 1, \dots, 7$ , by using the considered reconstruction operators, Lagrange PPH, PPHT with  $\epsilon = 0.5$ , PPHT with  $\epsilon = 0.05$ , and PPHT with adapted  $\epsilon_j$  in the region  $A_0$ .

Approximation errors in $A_0$					
$k$	Lagrange	PPH	PPHT, $\epsilon = 0.5$	PPHT, $\epsilon = 0.05$	PPHT, $\epsilon_j$
$k = 0$	5.6495	5.0072	4.8870	4.9125	4.9153
$k = 1$	9.4448	9.3051	9.1754	9.1740	9.1738
$k = 2$	9.3578	9.3588	9.5194	9.5194	9.5195
$k = 3$	9.3587	9.3591	9.5207	9.5208	9.5208
$k = 4$	9.3591	9.3593	9.5214	9.5214	9.5214
$k = 5$	9.3593	9.3594	9.5217	9.5217	9.5217
$k = 6$	9.3594	9.3595	9.5219	9.5219	9.5219
$k = 7$	9.3595	9.3595	9.5220	9.5220	9.5220
Approximation orders in $A_0$					
$k$	Lagrange	PPH	PPHT, $\epsilon = 0.5$	PPHT, $\epsilon = 0.05$	PPHT, $\epsilon_j$
$k = 1$	$-7.4 \times 10^{-1}$	$-8.9 \times 10^{-1}$	$-9.1 \times 10^{-1}$	$-9.0 \times 10^{-1}$	$-9.0 \times 10^{-1}$
$k = 2$	$1.3 \times 10^{-2}$	$-8.3 \times 10^{-3}$	$-5.3 \times 10^{-2}$	$-5.3 \times 10^{-2}$	$-5.3 \times 10^{-2}$
$k = 3$	$-1.3 \times 10^{-4}$	$-5.4 \times 10^{-5}$	$-2.1 \times 10^{-4}$	$-2.0 \times 10^{-4}$	$-2.0 \times 10^{-4}$
$k = 4$	$6.5 \times 10^{-5}$	$-2.9 \times 10^{-5}$	$-1.0 \times 10^{-4}$	$-9.9 \times 10^{-5}$	$-9.9 \times 10^{-5}$
$k = 5$	$3.3 \times 10^{-5}$	$-1.5 \times 10^{-5}$	$-5.0 \times 10^{-5}$	$-5.0 \times 10^{-5}$	$-4.9 \times 10^{-5}$
$k = 6$	$1.6 \times 10^{-5}$	$-7.4 \times 10^{-6}$	$-2.4 \times 10^{-5}$	$-2.5 \times 10^{-5}$	$-2.4 \times 10^{-5}$
$k = 7$	$8.1 \times 10^{-6}$	$-3.7 \times 10^{-6}$	$-1.2 \times 10^{-5}$	$-1.2 \times 10^{-5}$	$-1.2 \times 10^{-5}$

Then, we compute the numerical approximation order as,

$$p = \log_2 \frac{E_{k-1}}{E_k}, \quad k = 1, \dots, 7.$$

Notice that due to [Theorem 1](#) we can assume that for fine enough grids,

$$E_k \approx C (h^k)^p, \quad \text{with } h^k := \max_{i \in I_k \setminus \{0\}} h_i^k, \quad h_i^k := x_i^k - x_{i-1}^k, \quad h^k = \frac{h^{k-1}}{2}.$$

In [Tables 1, 2, 3, 4, 5](#) we present the errors committed by the considered reconstruction operators, and their corresponding approximation orders. We have used as initial nodes the defined nested grids  $X^k$ . The errors and orders appear separately for each kind of region  $A_0, A_1, A_2, A_3$  and  $A_4$ .

In [Table 1](#), we can see that neither of these methods is designed to adapt in the interval containing the jump discontinuity since it is impossible to localize exactly the discontinuity just working with the point values of the function. The largest error comes near the jump discontinuity for Lagrange reconstruction, as it can be observed in the column corresponding to this reconstruction. In the region  $A_1$  all the reconstruction operators attain fourth order of accuracy,  $p = 4$ , as it can be seen in [Table 2](#). Regions  $A_2$  and  $A_3$  correspond to the vicinity of an inflection point, where the nonlinear PPH reconstruction operator reduces the approximation order to third order. We can observe in [Tables 3, 4](#), how all the translated versions get closer to fourth order in these two regions,  $A_2$  and  $A_3$ . Albeit, the version with larger  $\epsilon$  and adapted  $\epsilon_j$  perform in a better way than with smaller  $\epsilon$  in these cases. Finally, in [Table 5](#) we can see how the nonlinear reconstruction operators reach second-order of accuracy in the intervals to the right and the left of the interval containing the jump discontinuity, while the linear Lagrange reconstruction operator completely loses the order of approximation. In the case of the adapted translated version, we get third-order due to the observation given in [Remark 3](#).

In [Fig. 1](#), we plot the function  $f(x)$  and the Lagrange, and PPHT (with  $\epsilon_j$  adapted) reconstructions obtained from the initial grids  $X^k, k = 0, 1, 2$ . We can see that around the singularity, Lagrange reconstruction loses the approximation order and the Gibbs phenomena appear. In this zone, PPHT reconstruction performs more properly, avoiding any Gibbs effects. We can see that no oscillations appear in the PPHT reconstruction even for the coarsest grid. These observations can be seen more clearly in [Fig. 2](#), where we have plotted a zoom of this region for  $k = 3$  for both operators Lagrange and  $PPHT$ . We also point out that the oscillations due to the jump discontinuity in Lagrange reconstruction do not diminish to zero with the subdivision level.

**Table 2**

Approximation errors  $E_k$  and approximation orders  $p$  in the infinity norm obtained at iteration  $k, k = 1, \dots, 7$ , by using the considered reconstruction operators, Lagrange PPH, PPHT with  $\epsilon = 0.5$ , PPHT with  $\epsilon = 0.05$ , and PPHT with adapted  $\epsilon_j$  in the region  $A_1$ .

Approximation errors in $A_1$					
$k$	Lagrange	PPH	PPHT, $\epsilon = 0.5$	PPHT, $\epsilon = 0.05$	PPHT, $\epsilon_j$
$k = 0$	3.7038	$1.9182 \times 10^{-2}$	$1.4586 \times 10^{-1}$	$2.7869 \times 10^{-2}$	$4.4601 \times 10^{-2}$
$k = 1$	$7.3685 \times 10^{-4}$	$6.5968 \times 10^{-3}$	$1.4201 \times 10^{-3}$	$4.6348 \times 10^{-3}$	$9.5688 \times 10^{-4}$
$k = 2$	$6.2735 \times 10^{-5}$	$8.3401 \times 10^{-4}$	$9.4378 \times 10^{-5}$	$4.5210 \times 10^{-4}$	$6.9863 \times 10^{-5}$
$k = 3$	$4.0575 \times 10^{-6}$	$3.4729 \times 10^{-5}$	$5.8493 \times 10^{-6}$	$2.2392 \times 10^{-5}$	$4.4229 \times 10^{-6}$
$k = 4$	$2.5733 \times 10^{-7}$	$2.6086 \times 10^{-6}$	$3.6925 \times 10^{-7}$	$1.5670 \times 10^{-6}$	$2.7765 \times 10^{-7}$
$k = 5$	$1.5978 \times 10^{-8}$	$1.8126 \times 10^{-7}$	$2.3181 \times 10^{-8}$	$1.0414 \times 10^{-7}$	$1.7329 \times 10^{-8}$
$k = 6$	$1.0021 \times 10^{-9}$	$1.0730 \times 10^{-8}$	$1.4459 \times 10^{-9}$	$6.3099 \times 10^{-9}$	$1.0840 \times 10^{-9}$
$k = 7$	$6.2737 \times 10^{-11}$	$6.5331 \times 10^{-10}$	$9.0272 \times 10^{-11}$	$3.8843 \times 10^{-10}$	$6.7782 \times 10^{-11}$
Approximation orders in $A_1$					
$k$	Lagrange	PPH	PPHT, $\epsilon = 0.5$	PPHT, $\epsilon = 0.05$	PPHT, $\epsilon_j$
$k = 1$	12.2953	1.5399	6.6824	2.5881	5.5426
$k = 2$	3.5540	2.9836	3.9114	3.3578	3.7757
$k = 3$	3.9506	4.5859	4.0121	4.3356	3.9815
$k = 4$	3.9789	3.7348	3.9856	3.8369	3.9937
$k = 5$	4.0094	3.8472	3.9935	3.9115	4.0019
$k = 6$	3.9950	4.0784	4.0030	4.0447	3.9987
$k = 7$	3.9976	4.0377	4.0015	4.0219	3.9994

**Table 3**

Approximation errors  $E_k$  and approximation orders  $p$  in the infinity norm obtained at iteration  $k, k = 1, \dots, 7$ , by using the considered reconstruction operators, Lagrange PPH, PPHT with  $\epsilon = 0.5$ , PPHT with  $\epsilon = 0.05$ , and PPHT with adapted  $\epsilon_j$  in the region  $A_2$ .

Approximation errors in $A_2$					
$k$	Lagrange	PPH	PPHT, $\epsilon = 0.5$	PPHT, $\epsilon = 0.05$	PPHT, $\epsilon_j$
$k = 0$	$7.5463 \times 10^{-1}$	$8.3447 \times 10^{-3}$	$2.3123 \times 10^{-2}$	$5.6651 \times 10^{-3}$	$2.9178 \times 10^{-3}$
$k = 1$	$4.2214 \times 10^{-5}$	$7.8190 \times 10^{-4}$	$1.9193 \times 10^{-4}$	$6.4427 \times 10^{-4}$	$6.7164 \times 10^{-5}$
$k = 2$	$3.4996 \times 10^{-6}$	$2.4763 \times 10^{-4}$	$1.8960 \times 10^{-5}$	$1.0918 \times 10^{-4}$	$5.3926 \times 10^{-6}$
$k = 3$	$3.0851 \times 10^{-7}$	$3.0993 \times 10^{-5}$	$1.2028 \times 10^{-6}$	$8.7545 \times 10^{-6}$	$4.8008 \times 10^{-7}$
$k = 4$	$2.2334 \times 10^{-8}$	$3.8754 \times 10^{-6}$	$7.5666 \times 10^{-8}$	$6.3675 \times 10^{-7}$	$3.3935 \times 10^{-8}$
$k = 5$	$1.4894 \times 10^{-9}$	$4.8446 \times 10^{-7}$	$4.7431 \times 10^{-9}$	$4.3337 \times 10^{-8}$	$2.2339 \times 10^{-9}$
$k = 6$	$9.5977 \times 10^{-11}$	$6.0559 \times 10^{-8}$	$2.9687 \times 10^{-10}$	$2.8345 \times 10^{-9}$	$1.4299 \times 10^{-10}$
$k = 7$	$6.0880 \times 10^{-12}$	$7.5699 \times 10^{-9}$	$1.8566 \times 10^{-11}$	$1.8137 \times 10^{-10}$	$9.040 \times 10^{-12}$
Approximation orders in $A_2$					
$k$	Lagrange	PPH	PPHT, $\epsilon = 0.5$	PPHT, $\epsilon = 0.05$	PPHT, $\epsilon_j$
$k = 1$	14.1257	3.4158	6.9126	3.1364	5.4411
$k = 2$	3.5925	1.6588	3.3395	2.5609	3.6386
$k = 3$	3.5038	2.9982	3.9784	3.6406	3.4896
$k = 4$	3.7880	2.9995	3.9907	3.7812	3.8224
$k = 5$	3.9064	2.9999	3.9957	3.8770	3.9251
$k = 6$	3.9559	3.0000	3.9980	3.9344	3.9655
$k = 7$	3.9787	3.0000	3.9990	3.9661	3.9835

In Fig. 3, we analyze the numerical behavior of the truncation parameter  $\epsilon$  and the effect of the parameter  $\beta$  introduced in its definition. As we can see the large values of  $\epsilon$  correspond with the areas around the inflection points of the function and the parameter takes values very close to  $\epsilon = 0$  in the three intervals around the jump discontinuity. The effect of  $\beta$  is more noticeable as we increase its value from  $\beta = 1$  to  $\beta = 100$ , setting the value of the parameter  $\epsilon$  closer to zero for the smooth areas without inflection points. This fact makes the translated version of this reconstruction similar to the original PPH reconstruction operator in smooth convex areas.

**Table 4**

Approximation errors  $E_k$  and approximation orders  $p$  in the infinity norm obtained at iteration  $k, k = 1, \dots, 7$ , by using the considered reconstruction operators, Lagrange PPH, PPHT with  $\epsilon = 0.5$ , PPHT with  $\epsilon = 0.05$ , and PPHT with adapted  $\epsilon_j$  in the region  $A_3$ .

Approximation errors in $A_3$					
$k$	Lagrange	PPH	PPHT, $\epsilon = 0.5$	PPHT, $\epsilon = 0.05$	PPHT, $\epsilon_j$
$k = 0$	$6.3455 \times 10^{-4}$	$2.2239 \times 10^{-3}$	$1.2150 \times 10^{-3}$	$1.9915 \times 10^{-3}$	$8.6245 \times 10^{-4}$
$k = 1$	$9.0640 \times 10^{-5}$	$2.9306 \times 10^{-4}$	$1.4797 \times 10^{-4}$	$2.5484 \times 10^{-4}$	$1.1640 \times 10^{-4}$
$k = 2$	$9.2479 \times 10^{-6}$	$3.4429 \times 10^{-5}$	$1.6629 \times 10^{-5}$	$3.0064 \times 10^{-5}$	$1.2170 \times 10^{-5}$
$k = 3$	$6.5454 \times 10^{-7}$	$2.7653 \times 10^{-6}$	$1.0760 \times 10^{-6}$	$2.3029 \times 10^{-6}$	$8.1262 \times 10^{-7}$
$k = 4$	$4.3080 \times 10^{-8}$	$2.0098 \times 10^{-7}$	$6.8410 \times 10^{-8}$	$1.6202 \times 10^{-7}$	$5.1976 \times 10^{-8}$
$k = 5$	$2.7567 \times 10^{-9}$	$4.3976 \times 10^{-8}$	$4.6111 \times 10^{-9}$	$2.2983 \times 10^{-8}$	$3.2797 \times 10^{-9}$
$k = 6$	$1.7424 \times 10^{-10}$	$4.6559 \times 10^{-9}$	$2.9178 \times 10^{-10}$	$1.8210 \times 10^{-9}$	$2.0587 \times 10^{-10}$
$k = 7$	$1.0951 \times 10^{-11}$	$5.0457 \times 10^{-10}$	$1.8375 \times 10^{-11}$	$1.3610 \times 10^{-10}$	$1.2895 \times 10^{-11}$
Approximation orders in $A_3$					
$k$	Lagrange	PPH	PPHT, $\epsilon = 0.5$	PPHT, $\epsilon = 0.05$	PPHT, $\epsilon_j$
$k = 1$	2.8075	2.9238	3.0376	2.9662	2.8893
$k = 2$	3.2929	3.0895	3.1535	3.0835	3.2577
$k = 3$	3.8206	3.6381	3.9500	3.7065	3.9046
$k = 4$	3.9254	3.7823	3.9753	3.8291	3.9667
$k = 5$	3.9660	2.1923	3.8910	2.8176	3.9862
$k = 6$	3.9838	3.2396	3.9821	3.6578	3.9937
$k = 7$	3.9919	3.2059	3.9891	3.7420	3.9969

**Table 5**

Approximation errors  $E_k$  and approximation orders  $p$  in the infinity norm obtained at iteration  $k, k = 1, \dots, 7$ , by using the considered reconstruction operators, Lagrange PPH, PPHT with  $\epsilon = 0.5$ , PPHT with  $\epsilon = 0.05$ , and PPHT with adapted  $\epsilon_j$  in the region  $A_4$ .

Approximation errors in $A_4$					
$k$	Lagrange	PPH	PPHT, $\epsilon = 0.5$	PPHT, $\epsilon = 0.05$	PPHT, $\epsilon_j$
$k = 0$	$7.5463 \times 10^{-1}$	$7.3017 \times 10^{-3}$	$2.3122 \times 10^{-2}$	$4.9884 \times 10^{-3}$	$2.9178 \times 10^{-3}$
$k = 1$	$6.1204 \times 10^{-1}$	$2.3996 \times 10^{-3}$	$3.3130 \times 10^{-3}$	$4.8664 \times 10^{-4}$	$1.7116 \times 10^{-4}$
$k = 2$	$6.1887 \times 10^{-1}$	$6.1993 \times 10^{-4}$	$8.0841 \times 10^{-4}$	$9.8797 \times 10^{-5}$	$1.9854 \times 10^{-5}$
$k = 3$	$6.2234 \times 10^{-1}$	$1.5738 \times 10^{-4}$	$1.9971 \times 10^{-4}$	$2.2119 \times 10^{-5}$	$2.3812 \times 10^{-6}$
$k = 4$	$6.2409 \times 10^{-1}$	$3.9636 \times 10^{-5}$	$4.9635 \times 10^{-5}$	$5.2260 \times 10^{-6}$	$2.9126 \times 10^{-7}$
$k = 5$	$6.2496 \times 10^{-1}$	$9.9451 \times 10^{-6}$	$1.2372 \times 10^{-5}$	$1.2697 \times 10^{-6}$	$3.6003 \times 10^{-8}$
$k = 6$	$6.2540 \times 10^{-1}$	$2.4908 \times 10^{-6}$	$3.0887 \times 10^{-6}$	$3.1290 \times 10^{-7}$	$4.4750 \times 10^{-9}$
$k = 7$	$6.2562 \times 10^{-1}$	$6.2325 \times 10^{-7}$	$7.7161 \times 10^{-7}$	$7.7664 \times 10^{-8}$	$5.5778 \times 10^{-10}$
Approximation orders in $A_4$					
$k$	Lagrange	PPH	PPHT, $\epsilon = 0.5$	PPHT, $\epsilon = 0.05$	PPHT, $\epsilon_j$
$k = 1$	0.3021	1.6054	2.8031	3.3577	4.0914
$k = 2$	-0.0160	1.9526	2.0350	2.3003	3.1078
$k = 3$	-0.0081	1.9779	2.0172	2.1591	3.0597
$k = 4$	-0.0040	1.9893	2.0085	2.0815	3.0314
$k = 5$	-0.0020	1.9948	2.0042	2.0412	3.0161
$k = 6$	-0.0010	1.9974	2.0021	2.0207	3.0082
$k = 7$	-0.0005	1.9987	2.0010	2.0104	3.0041

**Remark 5.** The numerical experiment has been carried out using a finite interval, that in principle, falls out from the scope of [Theorem 1](#). However, the results are also true for the finite case away from the boundaries, and the proof remains exactly the same. Notice that any finite discretization of a finite interval is a  $\sigma$  quasi-uniform grid according to [Definition 4](#). The boundaries have been treated by using non-centered third-degree Lagrange polynomials so that if we take into account that the discontinuity and the inflection point are placed far from the boundaries, they do not affect the attained numerical approximation order.

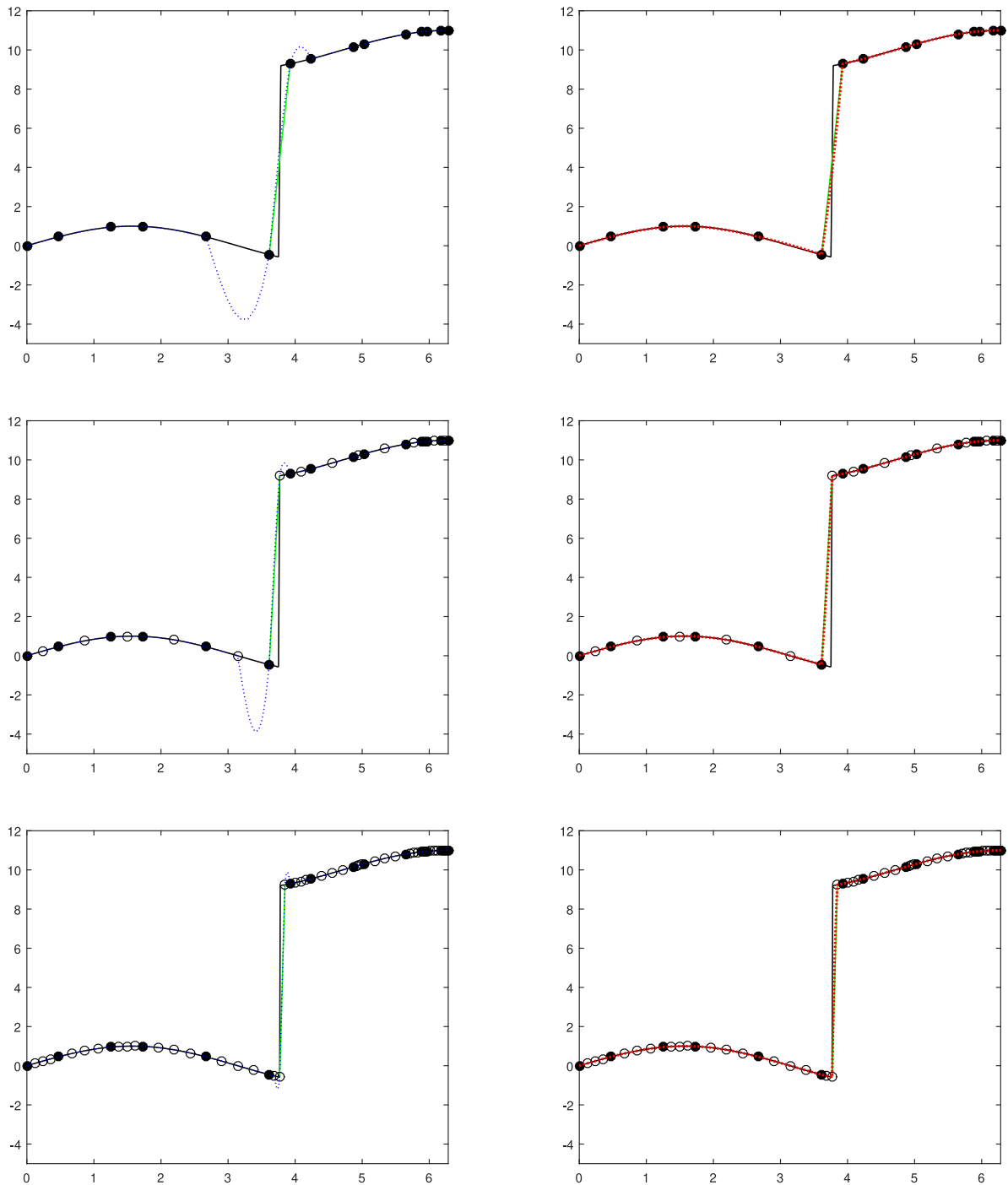


**Fig. 1.** In black solid line: function  $f(x)$ . In green solid line: the straight line joining the extreme points of the jump interval  $[x_j^k, x_{j+1}^k]$ . In blue dotted line: Lagrange reconstruction. In red dotted line: PPHT reconstruction with adapted  $\epsilon_j$ . Void circles stand for initial nodes, filled circles for nodes at the  $k$  subdivision level. Top-left: Lagrange  $k = 0$ , top-right: PPHT  $k = 0$ , middle-left: Lagrange  $k = 1$ , middle-right: PPHT  $k = 1$ , bottom-left: Lagrange  $k = 2$ , bottom-right: PPHT  $k = 2$ .

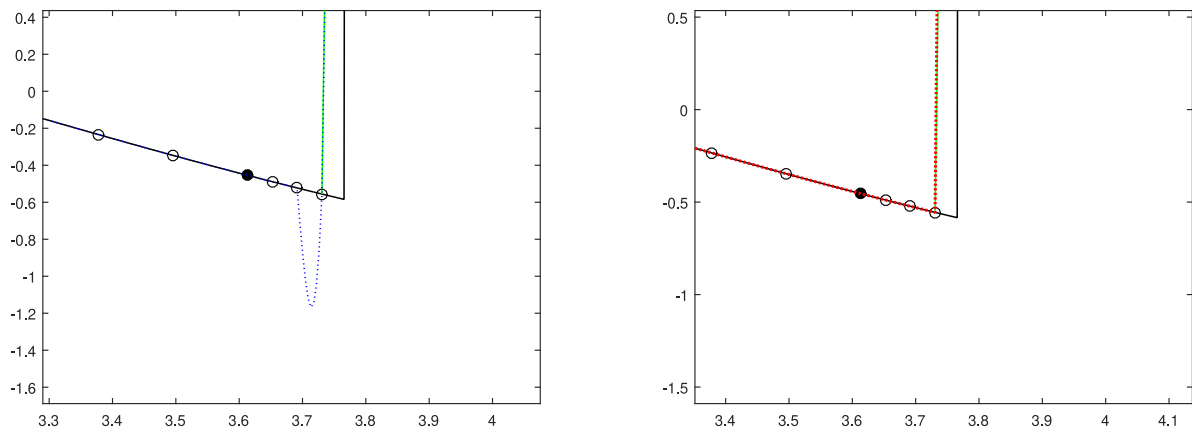


Fig. 2. Zoom of the region around the jump discontinuity for subdivision grid level  $k = 3$ . Left: Lagrange, right:  $PPHT$  with adapted  $\epsilon_j$ .

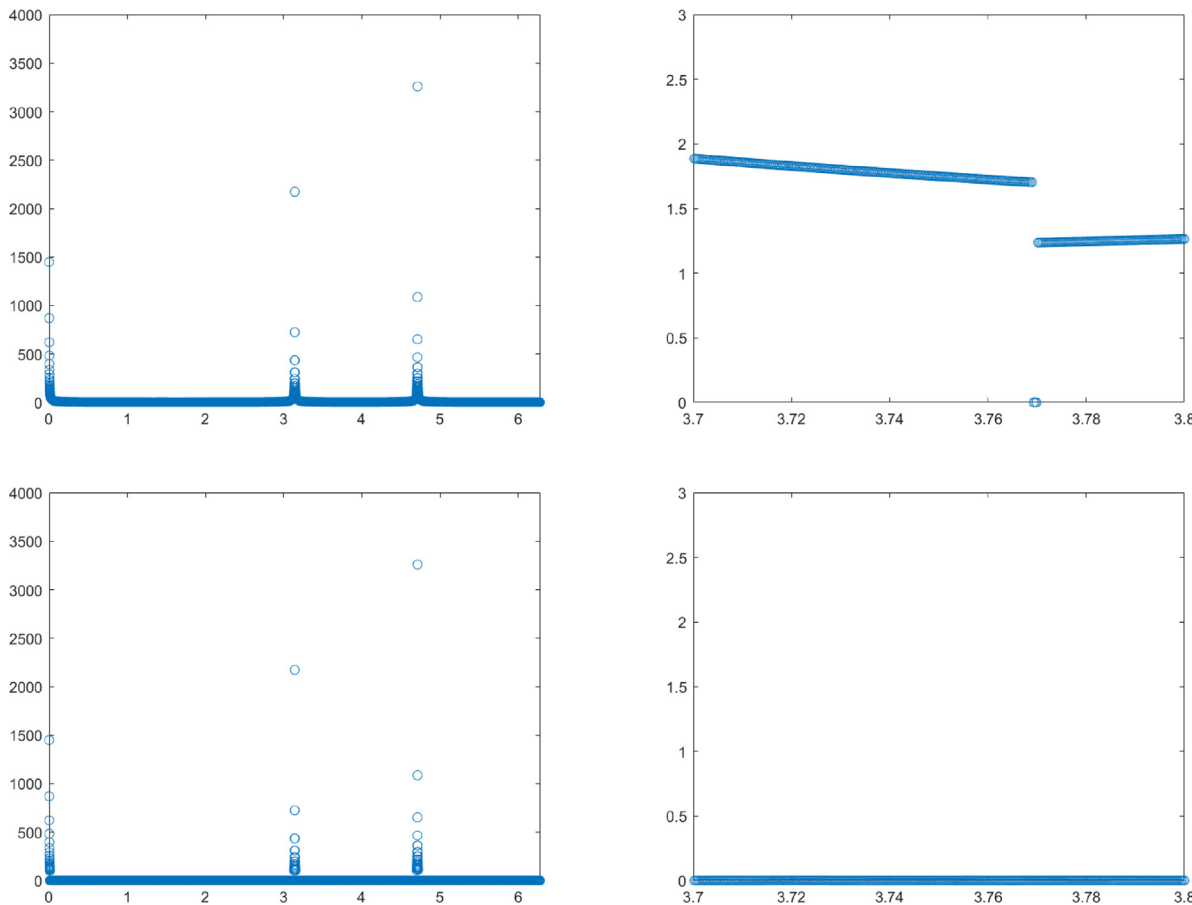


Fig. 3. Values of the  $\epsilon$  parameter in (19) along different intervals for the  $x$  variable. Top-left: for  $\beta = 1$  in the interval  $[0, 2\pi]$ , top-right: for  $\beta = 1$  in the interval  $[3.7, 3.8]$ , bottom-left: for  $\beta = 100$  in the interval  $[0, 2\pi]$ , bottom-right: for  $\beta = 100$  in the interval  $[3.7, 3.8]$ .

**Remark 6.** The presented translation strategy and the reconstruction operator used, both could be defined for functions with several variables in a nonseparable way, by observing the fact that, we need to define appropriate substitutes for divided differences, and we have to use a linear reconstruction method as the base method to be

written in terms of weighted arithmetic means of the defined divided differences. These weighted arithmetic means will be in turn replaced by adequate translated nonlinear weighted means. The authors are working to develop such a scheme for two dimensional functions in triangular meshes.

## 6. Conclusions

Using the general definition of a translation operator given in [9], and previously mentioned in [5], we have considered several specific cases. In particular, we have studied a way of choosing a translation adaptively depending on the specific data to which it is going to be applied. In turn, this translation operator has been used to extend the definition of the already existing PPH reconstruction operator on nonuniform grids [22,23] to work appropriately with functions that are not necessarily strictly convex. We give a corresponding theorem ensuring the pursued objective of getting fourth-order of approximation at the smooth parts of the function, independently of the presence or not of inflection points. Finally, we have performed some numerical experiments to check the behavior of the proposed adaptation.

## References

- [1] T. Ahancaou, A. Ikemakhen, Hyperbolic interpolatory geometric subdivision schemes, *J. Comput. Appl. Math.* 399 (2022) 22, Paper No. 113716.
- [2] S. Amat, F. Aràndiga, A. Cohen, R. Donat, Tensor product multiresolution analysis with error control for compact image representation, *Signal Process.* 82 (4) (2002) 587–608.
- [3] S. Amat, F. Aràndiga, A. Cohen, R. Donat, G. Garcia, M. von Oehsen, Data compression with ENO schemes: a case study, *Appl. Comput. Harmon. Anal.* 11 (2) (2001) 273–288.
- [4] S. Amat, K. Dadourian, J. Liandrat, J.C. Trillo, High order nonlinear interpolatory reconstruction operators and associated multiresolution schemes, *J. Comput. Appl. Math.* 253 (2013) 163–180.
- [5] S. Amat, R. Donat, J. Liandrat, J.C. Trillo, Analysis of a new nonlinear subdivision scheme. Applications in image processing, *Found. Comput. Math.* 6 (2) (2006) 193–225.
- [6] S. Amat, R. Donat, J.C. Trillo, Proving convexity preserving properties of interpolatory subdivision schemes through reconstruction operators, *Appl. Math. Comput.* 219 (14) (2013) 7413–7421.
- [7] S. Amat, J. Liandrat, On the stability of PPH nonlinear multiresolution, *Appl. Comput. Harmon. Anal.* 18 (2) (2005) 198–206.
- [8] S. Amat, P. Ortiz, J. Ruiz, J.C. Trillo, D.F. Yáñez, Geometric representation of the weighted harmonic mean of  $n$  positive values and potential uses, submitted for publication.
- [9] S. Amat, C.W. Shu, J. Ruiz, J.C. Trillo, On a class of splines free of Gibbs phenomenon, *Math. Modell. Numer. Anal.* 55 (2021) S29–S64.
- [10] F. Aràndiga, A. Cohen, R. Donat, N. Dyn, B. Basarab, Approximation of piecewise smooth functions and images by edge-adapted (ENO-EA) nonlinear multiresolution techniques, *Appl. Comput. Harmon. Anal.* 24 (2) (2008) 225–250.
- [11] M. Aslam, A family of 5-point nonlinear ternary interpolating subdivision schemes with  $C^2$  smoothness, *Math. Comput. Appl.* 23 (2) (2018) 8, Paper No. 18.
- [12] I. Cravero, M. Semplice, G. Visconti, Optimal definition of the nonlinear weights in multidimensional central WENOZ reconstructions, *SIAM J. Numer. Anal.* 57 (5) (2019) 2328–2358.
- [13] N. Dyn, E. Farkhi, S. Keinan, Approximation of 3D objects by piecewise linear geometric interpolants of their 1D cross-sections, *J. Comput. Appl. Math.* 368 (2020) 112466–112475.
- [14] N. Dyn, J.A. Gregori, D. Levin, A 4-point interpolatory subdivision scheme for curve design, *Comput. Aided Geom. Design* 4 (1987) 257–268.
- [15] N. Dyn, F. Kuijt, D. Levin, R. van Damme, Convexity preservation of the four-point interpolatory subdivision scheme, *Comput. Aided Geom. Design* 16 (8) (1999) 789–792.
- [16] V. Elling, Lax–Wendroff type theorem for unstructured quasi-uniform grids, *Math. Comp.* 76 (257) (2007) 251–272.
- [17] M.S. Floater, C.A. Michelli, Nonlinear stationary subdivision, in: N.K. Govil, N. Mohapatra, Z. Nashed, A. Sharma, J. Szabados (Eds.), *Approximation Theory: In Memory of A.K. Varna, 1998*, pp. 209–224.
- [18] T. Hang, Y. Zhai, Z. Zhou, W. Zhao, Conservative characteristic finite difference method based on ENO and WENO interpolation for 2D convection–diffusion equations, *J. Comput. Appl. Math.* 40 (6) (2021) 21, Paper No. 202.
- [19] S.I. Kabanikhin, O.I. Krivorotko, An algorithm for source reconstruction in nonlinear shallow-water equations, *Comput. Math. Math. Phys.* 58 (8) (2018) 1334–1343.
- [20] Z. Kui, J. Baccou, J. Liandrat, On the construction of multiresolution analyses associated to general subdivision schemes, *Math. Comp.* 90 (331) (2021) 2185–2208.
- [21] F. Kuijt, R. van Damme, Convexity preserving interpolatory subdivision schemes, *Const. Approx.* 14 (1998) 609–630.
- [22] P. Ortiz, J.C. Trillo, On the convexity preservation of a quasi  $C^3$  nonlinear interpolatory reconstruction operator on  $\sigma$  quasi-uniform grids, *Mathematics* 9 (4) (2021) 310, <http://dx.doi.org/10.3390/math9040310>.



- [23] P. Ortiz, J.C. Trillo, A piecewise polynomial harmonic nonlinear interpolatory reconstruction operator on nonuniform grids- adaptation around jump discontinuities and elimination of Gibbs phenomenon, *Mathematics* 9 (4) (2021) 335, <http://dx.doi.org/10.3390/math9040335>.
- [24] C.W. Shu, S. Osher, Efficient implementation of essentially non-oscillatory shock-capturing schemes, *J. Comput. Phys.* 77 (2) (1988) 439–471.
- [25] J.C. Trillo, *Nonlinear Multiresolution and Applications in Image Processing*, PhD in the University of Valencia, Spain, 2007.